


RESEARCH

Open Access



Experimental Research on Bond Behaviour of Fabric Reinforced Cementitious Matrix Composites for Retrofitting Masonry Walls

Fayu Wang^{1*} , Nicholas Kyriakides^{2*}, Christis Chrysostomou³, Eleftherios Eleftheriou⁴, Renos Votsis⁵ and Rogiros Illampas⁶

Abstract

Fabric reinforced cementitious matrix (FRCM) composites, also known as textile reinforced mortars (TRM), an inorganic matrix constituting fibre fabrics and cement-based mortar, are becoming a widely used composite material in Europe for upgrading the seismic resistance of existing reinforced concrete (RC) frame buildings. One way of providing seismic resistance upgrading is through the application of the proposed FRCM system on existing masonry infill walls to increase their stiffness and integrity. To examine the effectiveness of this application, the bond characteristics achieved between (a) the matrix and the masonry substrate and (b) the fabric and the matrix need to be determined. A series of experiments including 23 material performance tests, 15 direct tensile tests of dry fabric and composites, and 30 shear bond tests between the matrix and brick masonry, were carried out to investigate the fabric-to-matrix and matrix-to-substrate bond behaviour. In addition, different arrangements of extruded polystyrene (XPS) plates were applied to the FRCM to test the shear bond capacity of this insulation system when used on a large-scale wall.

Keywords: cementitious composite materials, fabric reinforced cementitious matrix, fibre fabric, textile reinforced mortars, seismic resistance upgrading, bond behaviour, retrofitting masonry walls

1 Introduction

Fabric reinforced cementitious matrix (FRCM) (AC434 I, 2013; ACI Committee 549, 2013) composites comprising an inorganic matrix of fibre fabrics and cement-based mortar are widely used in the retrofitting of existing reinforced concrete (RC) buildings. This system is generally known as textile reinforced mortar (TRM), and it is applied on different substrates for structural reinforcement. Moreover, the principle of FRCM composites is to

employ a mineral-based material as the bonding agent to embed the fibre material—thus it has also been considered as a type of mineral-based composite (MBC) material (Blanksvärd et al., 2009; Orosz et al., 2010).

Owing to its exceptional compatibility with substrates, its reversibility, vapour permeability, good resistance to high temperatures, and durability against detrimental agents (Cagegi, Lanoye, et al., 2017), several researchers have proposed the use of the FRCM system as a substitute for fibre-reinforced polymers (FRPs) when retrofitting existing RC frames, providing a lighter structural frame upgrade. In recent years, a new system that combines the FRCM with traditional thermal insulation for retrofitting existing masonry walls in RC frames has been fabricated (Triantafyllou et al., 2017, 2018). In-plane loading tests and fire-resistant tests have already verified the feasibility of TRMs plus XPS overlays to simultaneously provide both structural and energy upgradation of

*Correspondence: Fayu_Wang@outlook.com; nicholas.kyriakides@cut.ac.cy

¹ Research Fellow, Department of Civil Engineering and Geomatics, Faculty of Engineering and Technology, Cyprus University of Technology, No. 30 Archiepiskopou Kyprianou Str., P.O. Box 50329, 3036 Limassol, Cyprus

² Lecturer, Department of Civil Engineering and Geomatics, Faculty of Engineering and Technology, Cyprus University of Technology, No. 30 Archiepiskopou Kyprianou Str., P.O. Box 50329, 3036 Limassol, Cyprus
Full list of author information is available at the end of the article
Journal information: ISSN 1976-0485 / eISSN 2234-1315

masonry walls. However, by treating the material properties of the matrix as variables, various levels of structural upgrading can be achieved. This outcome depends on the properties of the material itself, as well as on the bond between each element/layer (mortar–textile and mortar–masonry). Consideration of the bond between each layer extends to the insulating material, which makes the shear bond behaviour even more complicated. Therefore, the selection of the appropriate materials and the corresponding bond mechanisms within layers forms the basis of further research herein, which will help in building new retrofitting system for masonry walls.

During the last decade, research on the topic of FRCM composites focused on the improvement of the material properties and the application processes. As the primary load-bearing element for tensile force, fabrics have been refined to provide the required levels of tensile strength and elasticity. It has been concluded that the tensile performance of the textile depends on the tensile strength of the fibres and the amount and density of the threads (Butler et al., 2010; Scheffler et al., 2009a, b). Therefore, if enough threads are stressed in the direction of tension, sufficient load-bearing requirements can be provided without being restricted by the types of fibres. In addition, since the cords do not function in the force direction, they are not stressed when the main bundles are not dislocated, and the fibre count and density can be reduced for material saving. Unidirectional and quadri-axial meshes are not desirable because they cause material wastage, and their bearing capacity is not significantly improved (Cagegi, Lanoye, et al., 2017). Moreover, reducing the mesh size leads to a reduction in mechanical interlocking, which is not favourable to the bond behaviour. Furthermore, knitted and bonded cords, usually used as open constructions or meshes, cannot effectively transfer the shear of the cutting matrix to the main bundle. Therefore, woven grids can achieve better bonds and effectively reduce the slip of fabric in the matrix. Lastly, the long-term durability of the textile can be jeopardised by the corrosion of the alkaline mortar because the fibre is easily alkaline-corroded when it is immersed in the unhardened mortar or is in a humid environment. In order to improve durability, in addition to the use of alkali-resistant glass (ARG) fibres, other types of fabrics can also be utilised by sizing or coating with (nano-dispersed) polymers such as epoxy resin (Scheffler et al., 2009; Signorini et al., 2018). This not only improves the durability and stability of the fabric, but also allows for easier handling and installation. By changing the properties of the surface, it is also possible to enhance the chemical bond and friction, thereby reducing fabric sliding within the matrix.

As one of the essential components of the FRCM system, the mortar of the cementitious matrix provides the bonding effect between the substrate and the outer thermal insulation materials, and improves the co-operative working mechanism with the fabric. First, the bond strength between the substrate and the reinforced mortar benefits from the chemical bond, which depends on the tensile strength of the mortar, which itself depends on the particle diameter of the aggregate. Therefore, filling the cement and aggregate pores with admixture, which can reduce its porosity and make the interior of the cement mortar more compact, establishing a tighter chemical bond, is usually considered. Second, the addition of a polymer to the cement mortar improves workability, increases flexural and compressive strengths, and decreases water absorption, carbonation, and chloride ion penetration (Aggarwal et al., 2007). In addition, the appropriate addition of fibres can further improve the mechanical properties such as tensile and flexural strengths, and even enhance the ductility and resistance to shrinkage of the mortar (Krishnamurthy et al., 2017). Finally, strong permeability and fast hardening of the mortar is also needed for construction on vertical walls. Using a spray gun can directly transfer the mortar to the wall to meet the needs of rapid construction and repair damaged wall surfaces as well.

To achieve an effective combination of materials in the FRCM system, a multitude of experimental investigations has been carried out by more than 20 research teams in different European countries. Different types of fabrics embedded in various based mortars have been studied using direct tensile and shear bond tests. The results from these research studies have been categorised and organised into a more systematic set of test methods (Arboleda et al., 2016; De Felice et al., 2018; De Santis, Ceroni, et al., 2017; D3039/D3039M-17 2017). In most current studies, it is worth mentioning that rectangular prism specimens and dumbbell specimens have completely different results in the direct tensile test owing to their different shapes and gripping methods (D'Antino and Papanicolaou, 2018). In the shear bond tests on masonry substrates, the stress distribution was discontinuous owing to the anisotropy of the bricks and the interlocking effect provided by the mortar joints (De Felice et al., 2016). Insufficient embedded length of the fabric may change the failure modes of the test specimens, thereby determining a smaller bond strength result (Dalalbashi et al., 2018) and different failure mechanisms. The above influencing factors are considered in the current experimental research described herein. At the same time, the FRCM system has also received the research interest of Chinese scholars. Bond–slip behaviour of basalt textile meshes in

ultra-high ductility cementitious composites has been investigated by pull-out tests (Jiang et al., 2019). And it also showed that FRCM would have a good application prospect in China.

Overall, current state-of-the-art sorted out lessons from reviewing the latest research results (De Felice et al., 2020), it is time to integrate innovative materials and determine techniques to propose a holistic and novel methodology for simultaneous upgrading of both the seismic resistance and the energy efficiency of existing buildings, taking economic, technical, geo-location, durability, and environmental factors into account. Therefore, the study of the tensile and shear bond behaviours of FRCM composites for retrofitting masonry walls, particularly with thermal insulation layers added to the extensor of buildings, has become essential. To this end, a series of experiments including 23 material performance tests, 15 direct tensile tests on dry fabric and composites, and 30 shear bond tests between the matrix and brick masonry were carried out to investigate the fabric-to-matrix and matrix-to-substrate bond mechanisms. Finally, by understanding the different failure mechanisms of the specimens, the improvement of the test method and the matters needing attention in practical engineering applications on large-scale walls are proposed at the end of this paper.

2 Test Setup

A series of experiments including 23 material performance tests, 15 direct tensile tests on dry fabric and composites, and 30 shear bond tests between the matrix and brick masonry, were carried out at the Large Structures Laboratory of the Cyprus University of Technology. The materials used during the textile and mortar tests were consistent—that is, the same textile and mortar composition was used to ensure limited variation in material properties. Similarly, the dimensions of the specimens across tests were appropriate for comparison purposes.

2.1 Materials

2.1.1 Fabric (textile)

A commercial alkali-resistant (AR) styrene–butadiene rubber (SBR)-coated glass fibre fabric was used in Triantafyllou et al., (2018). The SBR coating not only results in excellent alkaline resistance of the fibres, but is also considered to have good abrasion resistance and heat-ageing properties. The fabric mesh has two orthogonal directions of glass fibre bunches of unequal quantity and spacing, as shown in Fig. 1a. Its raw weight was 280 g/m^2 . The vertical bundles (weft yarns) had a weight of 145 g/m^2 with a spacing of 14.2 mm, woven using horizontal cords (warp yarns) with a weight of 135 g/m^2 , spaced 18.1 mm

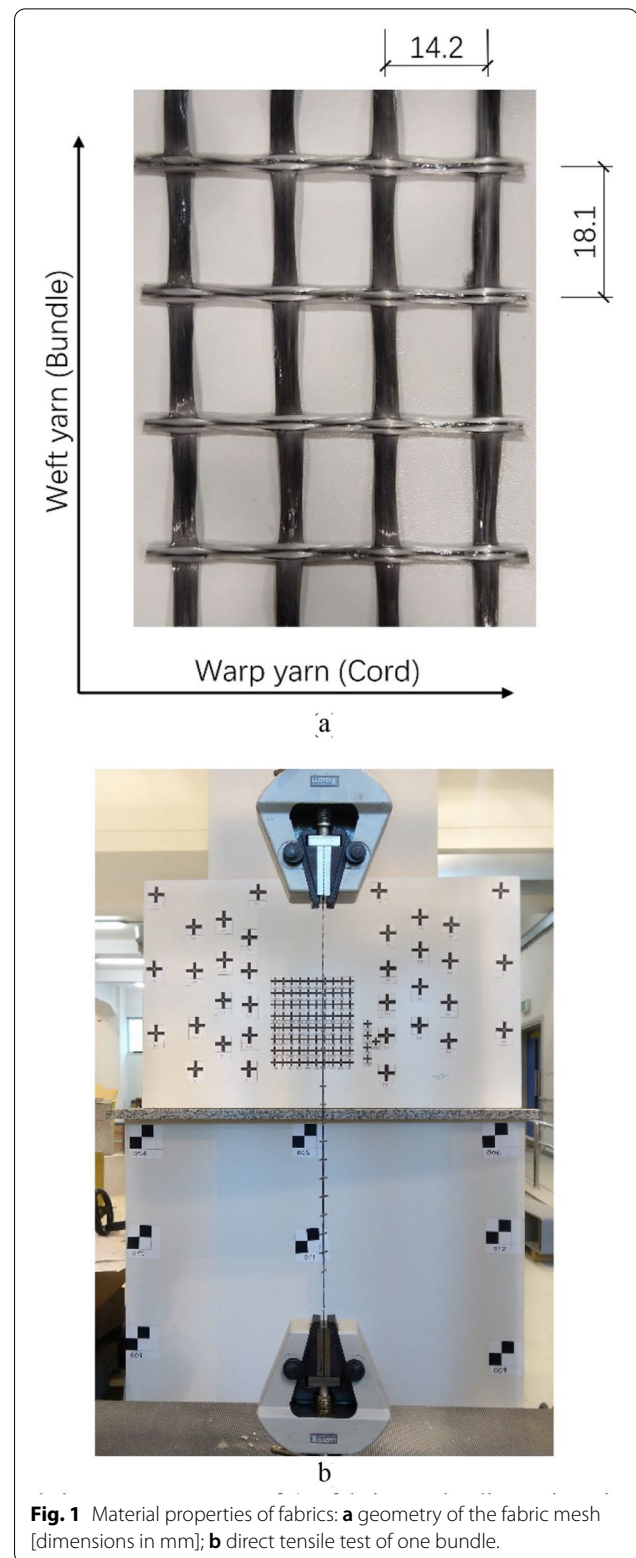


Fig. 1 Material properties of fabrics: **a** geometry of the fabric mesh [dimensions in mm]; **b** direct tensile test of one bundle.

apart. The total weight of the textile after surface treatment was 360 g/m^2 .

Although each bundle of fabric has the same number of fibres, the cross-sectional area of each bundle is not the same owing to manufacturing differences. Each bundle was tested under tensile force up to failure, as in Caggegi, Lanoye, et al. (2017)); Scheffler et al., (2009). The strength and deviation were evaluated by repeating tests five times, as shown in Fig. 1b. The position of the breaks of all five bundles was at the intersection of the weft and the warp. The average tensile breaking load of one bunch of the fabric was 579.36 N, the standard deviation was 11.63. This fabric has different fibre densities at the intersection and intermediate positions, and thus the cross-sectional area is also distinct. To facilitate the study of the relationship of strengths among different tests in this study, the cross-sectional area of each main bundle was taken to be 2 mm^2 to simplify the calculation. Therefore, the average tensile strength of the fabric was 289.68 MPa, its standard deviation was 5.81.

2.1.2 Cementitious Matrix (Mortar)

The cementitious matrix was made up of cement-based fibre-reinforced polymeric repair mortar. Each bag of this commercial mortar is packed with 25 kg of powder, which needs to be mixed with 4 kg of water as prescribed by the manufacturer. There are four reasons for choosing this type of mortar. It has high strength, mainly because it includes small glass fibres (higher tensile and flexural strength) which makes it suitable for the FRCM system.

Its durable abrasion and excellent resistance to water, oil, and non-aggressive chemicals make it possible to better protect internal materials, which gives durability to structures. It also meets the requirements of vertical wall construction owing to its fast hardening. Last but not least, the strong permeability and high adhesion of this mortar lead to better bond properties, particularly chemical bonds.

A total of nine rectangular prisms measuring $40 \times 40 \times 160 \text{ mm}$, which had been made using the tensile bond test specimens, were used for testing the mechanical properties of the matrix mortar. This measure was designed to follow the EN 1015–11 standard (Uni, 2019). The flexural tests adopted the 3-point bending method and the tensile tests were performed using a clamp—which was the same as the tensile bond tests for better comparison. Each type of experiment was carried out three times, as shown in Fig. 2. In addition, the six half-prisms from initial flexural tests were also tension tested as their strength might be lower than that of the full prisms. It is known that before the first crack occurs in the tensile bond test, the matrix itself is uncracked, and the tensile behaviour is governed by the mechanical properties of the matrix. However, the strength of the first crack is usually smaller than that of the mortar block. Therefore, the half-prism tensile tests were expected to find a correlation. The compression test adopted the longitudinal compression by using the whole blocks to imitate the stress situation of the FRCM layer

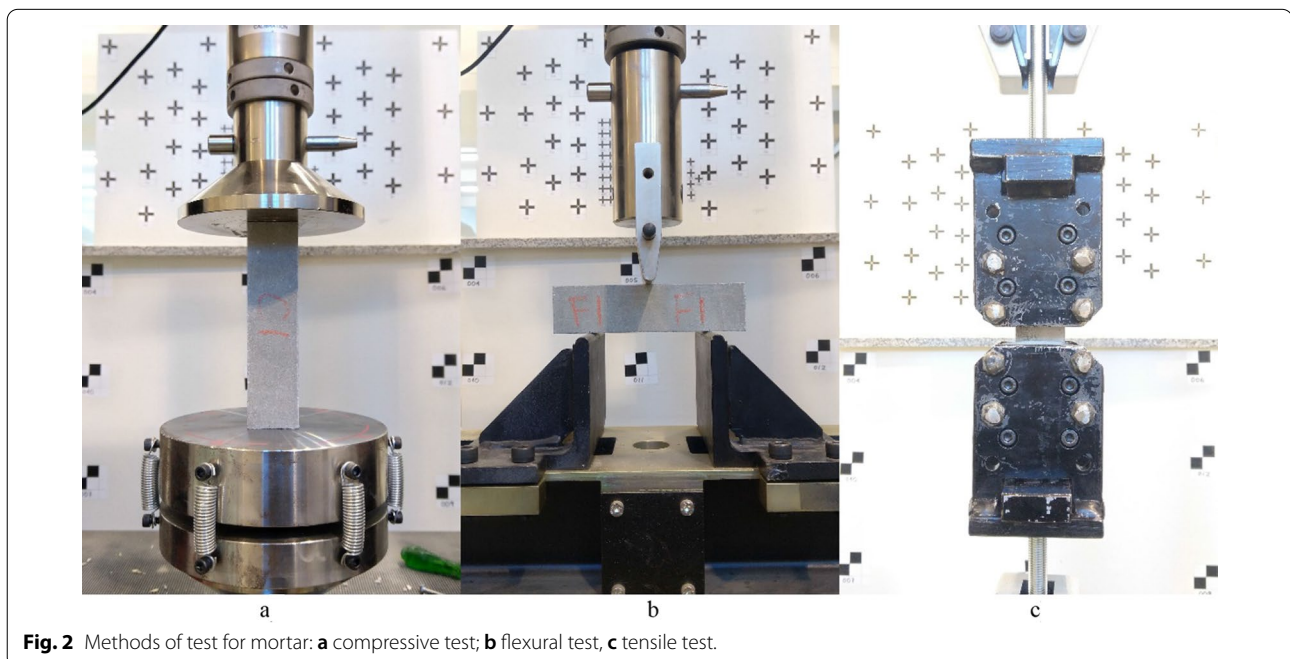


Table 1 Mechanical properties of mortar.

Type	Direction	No.	Peck load (N)	Strength (MPa)
Cementitious Matrix	C	1	86,347.00	53.97
		2	75,393.00	47.12
		3	80,277.00	50.17
		Avg	80,672.33	50.42
	F	1	2346.30	5.50
		2	2312.70	5.42
		3	2463.90	5.77
		Avg	2374.30	5.56
	T	1	2523.20	1.58
		2	2562.90	1.60
		3	2320.90	1.45
	Avg	2469.00	1.54	
	T (after F)	1	2132.40	1.33
2		2591.40	1.62	
3		2420.90	1.51	
4		2044.60	1.28	
5*		1645.70	1.03	
6		2499.50	1.56	
Avg		2337.76	1.46	
Mortar Joint	C	1	53,371.10	33.36
		2	55,385.36	34.62
		3	45,254.66	28.28
		Avg	51,337.04	32.09

* Denotes invalid data because of fast loading



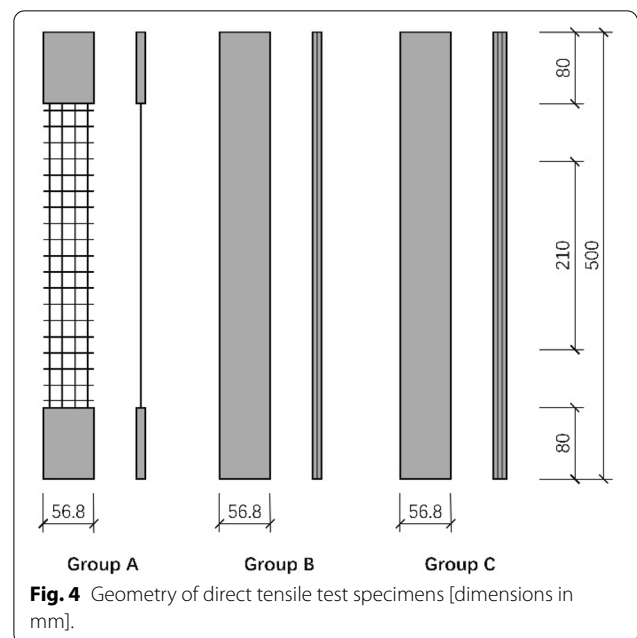
when the vertical wall was compressed. All the 28-day test strengths are shown in Table 1.

2.1.3 Other Materials

The masonry substrates for shear bond tests were made of hollow bricks (as in Fig. 3) of size 300 × 200 × 100 mm (length × width × height) typical of construction in the eastern Mediterranean. Because its light weight makes it suitable for earthquake resistance, its size is also the most common in the locality. The grooves on the brick surface may further enhance the mechanical interlocking with the FRCM interface. The water-to-cement-to-the sand ratio of the mortar joints was 4:7:21 by weight, where Type III Cement was used as a rapid hardening cement. Its compressive strength is shown in Table 1. Finally, extruded polystyrene (XPS) foam plates of 20 mm thickness were bonded to the outside of the matrix as a thermal insulation layer of the shear bond test specimens.

2.2 Specimen Design

The dimensions of the direct tensile test specimens are shown in Fig. 4. Group A specimens were made of a layer of dry fabric and two mortar-based gripping areas to avoid the influence of different transmission media on the stress transfer. The test specimens of Groups B and C were fabric reinforced cementitious matrices with one layer and two layers, respectively, of the textile inside. All samples were of the same length (500 mm) and width (56.8 mm), which was four times the warp spacing. In addition, all the thickness of the mortar on both sides of the fabric was designed to be 5 mm. The two layers of textile of Group C composites have been additionally added a 5-mm-thick layer of mortar. A 210-mm length in the



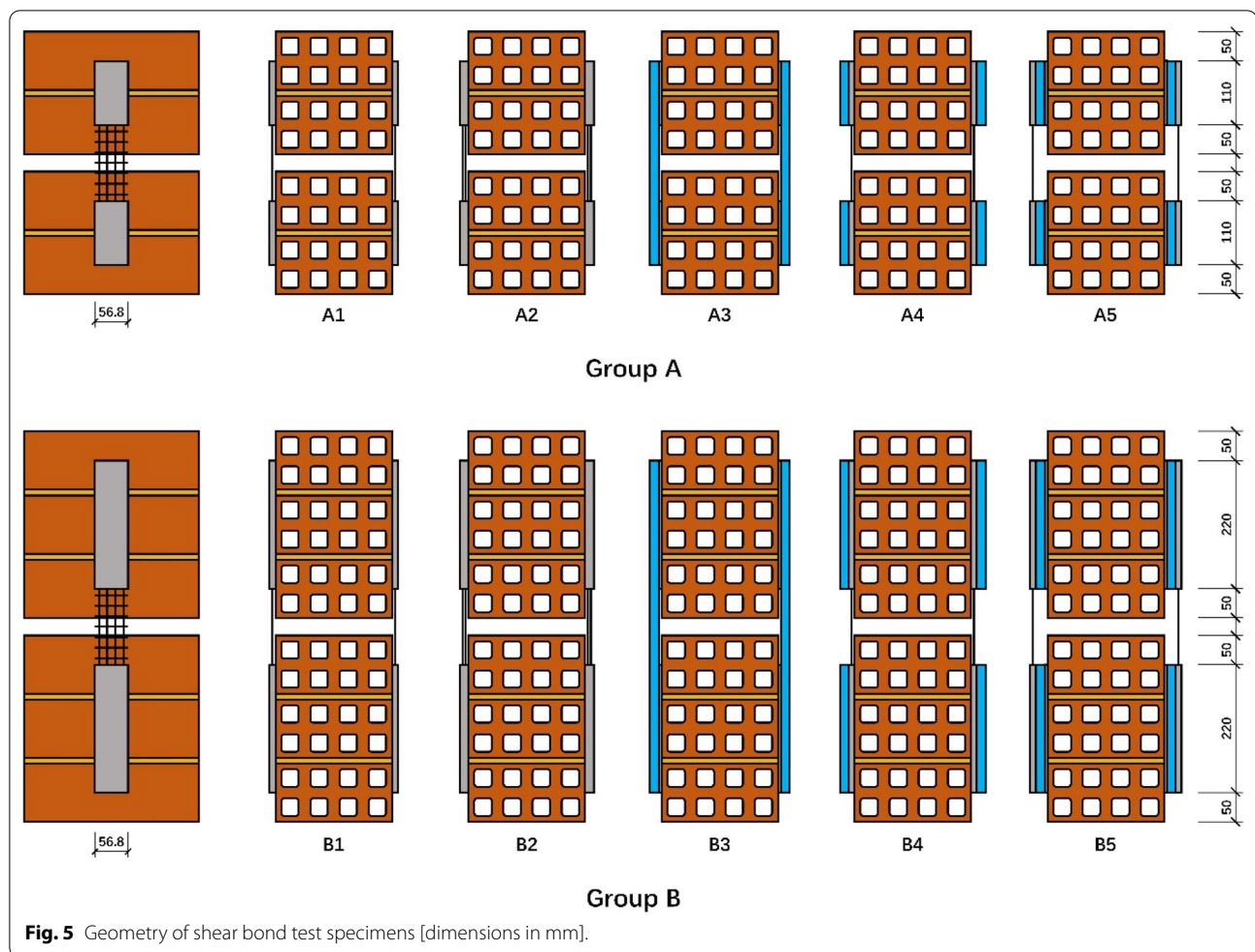


Fig. 5 Geometry of shear bond test specimens [dimensions in mm].

middle of each test specimen constituted the zone that was used as the basis for the displacement measurement.

To study the shear bond behaviour between the FRCM composites and the brick walls, two groups of double-lap double-prism test specimens were proposed. Five different settings for each group were designed to investigate the interfaces between the different materials. As shown in Fig. 5, the configuration of each test specimen was bilaterally symmetrical, the five different settings on one side were as follows: Setting 1—one layer of fabric embedded into two 10 mm thick cementitious matrices; Setting 2—two layers of fabric embedded into two 15-mm-thick cementitious matrices; Setting 3—one whole XPS plate fixed by two 5-mm-thick matrix mortar bonding areas; Setting 4—two XPS plates added on to the outsides of two identical matrices as in Setting 1; Setting 5—two XPS plates added on to the sides of two identical matrices as in Setting 1, fixed by two 5-mm-thick matrix mortar bonding areas.

One prism of the specimens of Group A had two bricks, while one of Group B had three; each mortar joint

had a thickness of 10 mm. The type of mortar joint was the flush joint, which is flat and level with the bricks—not only is this type of joint common, but the protruding portion of the extruded mortar joint may fall off and finally become a flush joint due to creep and long-term weathering. In addition, the use of this type of mortar joint helps in ignoring the mechanical interlocking effect of the matrix or mortar joint in the experiment and obtain the pure shear bond strength. All the matrices (and XPS plates) were placed in the middle of the masonry substrates to eliminate uneven stress distribution using the position of the mortar joints. The bonding areas of both groups were 56.8 mm wide, which was the same as for the tensile test specimens; their lengths were 110 mm for Group A and 220 mm for Group B, to study the effect of embedded length. In contrast, the length of 110 mm was equal to the height of one brick (100 mm) plus the thickness of a mortar joint (10 mm). Therefore, each bonding area of Group A specimens could be regarded as one bond unit that could be used to provide a parameter for

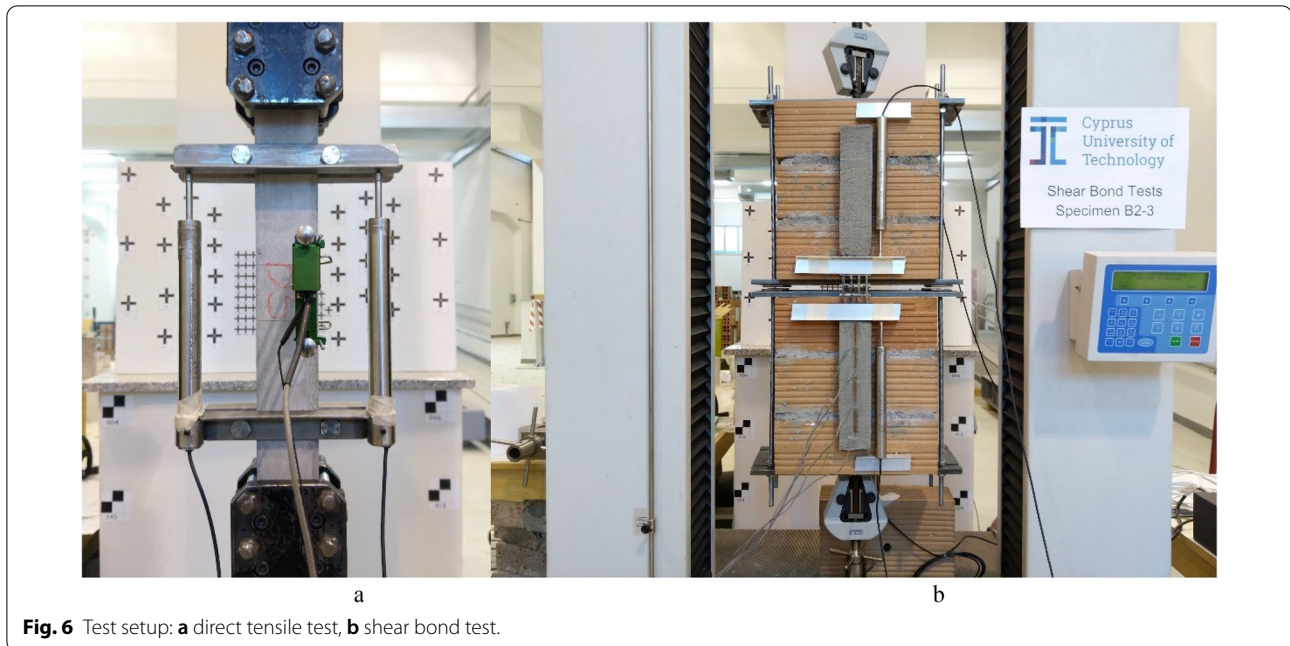


Fig. 6 Test setup: **a** direct tensile test, **b** shear bond test.

the simplified calculation and numerical simulation of large-scale walls.

2.3 Test Arrangement and Loading Procedures

The testing instruments are shown in Fig. 6. Direct tensile tests were carried out under displacement control using a tensile test machine at a loading rate of 0.5 mm/min. This rate appeared to be common in such experiments (D'Antino and Papanicolaou, 2018; Kim et al., 2018; Larrinaga et al., 2014). To investigate the maximum load-bearing capacity of the system, the clamping grips were not allowed to undergo torsional rotation to obtain the direct tensile strength of the composites. The gripping areas of the specimens were reinforced using soft sandpaper on both sides to eliminate slip and to prevent local stress concentration. Two frames made of angle steel were used to horizontally clamp the displacement test area. Then, two extensometers were symmetrically placed on the left and right sides and were secured parallel to the centre line of the test specimens. Each group of experiments was repeated five times, and a total of 15 samples were tested on the 28th day after curing.

As shown in Fig. 6b, the shear bond test specimens were fixed by upper and lower frames made of high-rigidity steel plates and threaded rods, and a vertical tensile load was applied using the test machine at a loading rate of 0.5 mm/min, which was the same as that used in the previous tensile bond tests. A 30-mm gap was reserved between the two symmetric prisms

of each specimen for mounting the pallets. Next, four aluminium alloy fixtures were set using fast-hardening glue and tape to clamp the unbonded areas of the fabric, which were close to the bonded regions. An extensometer was placed in parallel next to each bonded area to measure the loading end displacement. Five different settings for each group were repeated three times for a total of 30 specimens, all of which were tested after 28 days of production.

3 Test Results

3.1 Results of the Tensile Bond Tests

In Group A, the principal bundles of fabric had a minor slippage with the matrix at the initial stage of loading. However, when the tensile stress was transferred until the intersection with the first cord inside the matrix, the cord did not cut off the cement matrix because of the high-strength mortar used. Therefore, the dry fabric was not pulled out of the gripping areas, and finally ruptured at the intersection with the first cord. Due to the different section areas of the composite specimens, the average stress of Group A was converted using the same cross-sectional area as Group B; twice the peak force of Group A divided by the cross-sectional area of Group C is shown in Fig. 7, because of the two layers of fabric inside of Group C specimens.

The tensile bond behaviour of FRCM composites is usually described by the stress–strain curve. In this experiment, the curves could be characterised as exhibiting three-stage behaviour, which has been explained in

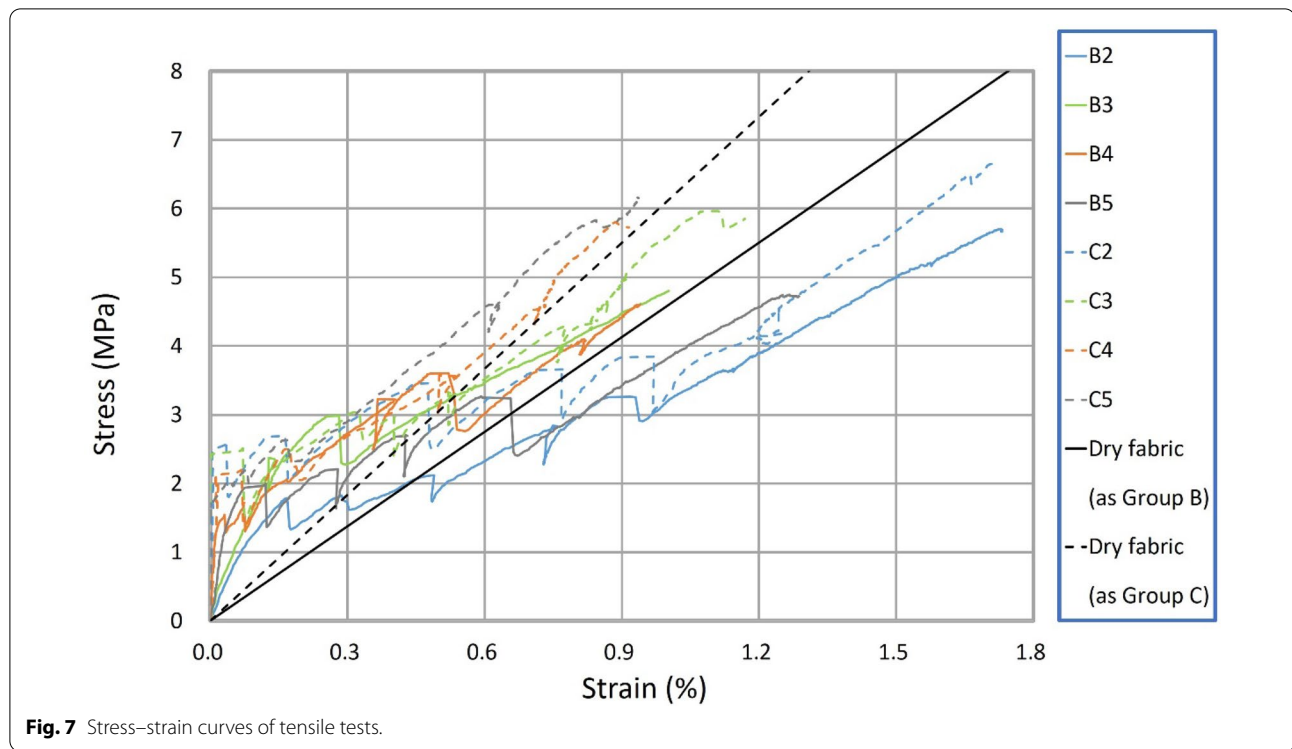


Table 2 Results of tensile bond tests.

Specimen	Stage I			Stage II			Stage III			No. of cracks
	σ_I (MPa)	ϵ_I (%)	EI (GPa)	σ_{II} (MPa)	ϵ_{II} (%)	EII (GPa)	σ_{III} (MPa)	ϵ_{III} (%)	EIII (GPa)	
B1	1.29	0.04	3.49	2.99	–	–	4.17	–	–	6
B2	1.79	0.17	1.06	2.92	0.94	0.15	5.70	1.73	0.35	5
B3*	2.37	0.14	1.70	2.46	0.77	0.01	4.80	1.00	0.99	4
B4	1.55	0.03	5.04	3.88	0.81	0.30	4.60	0.94	0.56	5
B5	2.00	0.12	1.65	2.96	0.81	0.14	4.74	1.27	0.39	5
C1	2.41	0.05	4.97	–	–	–	4.47	0.87	–	5
C2	2.63	0.03	7.61	4.12	1.20	0.13	6.67	1.71	0.49	5
C3	2.51	0.07	3.57	4.24	0.83	0.23	5.96	1.11	0.62	5
C4	2.09	–	–	4.35	0.71	0.32	5.80	0.89	0.83	6
C5	1.71	–	–	4.21	0.61	0.41	6.16	0.93	0.60	5

* Denotes invalid data due to a bending crack that occurred at the beginning because the specimen was not absolutely set upright

– Denotes lost data due to slippage that occurred because the specimens were not clamped tough

previous research (Caggegi, Lanoye, et al., 2017; Carozzi and Poggi, 2015; De Santis, Ceroni, et al., 2017; Arbolada et al., 2016; Ascione et al., 2015; De Santis and De Felice, 2015; Caggegi, Lanoye, et al., 2017; De Santis, Ceroni, et al., 2017). The test data are listed in Table 2; several values were lost, as explained below. In Stage I, the composites were uncracked, and the response was linear. Although the tensile behaviour is mainly governed by the mechanical properties of the matrix (Caggegi, Lanoye, et al., 2017), it also depends on the fabric as well

as on the fabric-to-matrix stress transfer (Ascione et al., 2015), which can lead to higher stress than the strength of the mortar itself. In addition, the test results of Group C showed a greater stiffness than that of Group B, not only because Group C samples used twice the fabric in only 1.5 times the cross-sectional area, but also because of the 5-mm spacing between the two layers of fabric can make the tensile forces of the two fabrics be independently transferred to the matrix. Therefore, it is expected to have a better fabric-to-matrix bond, more so via the

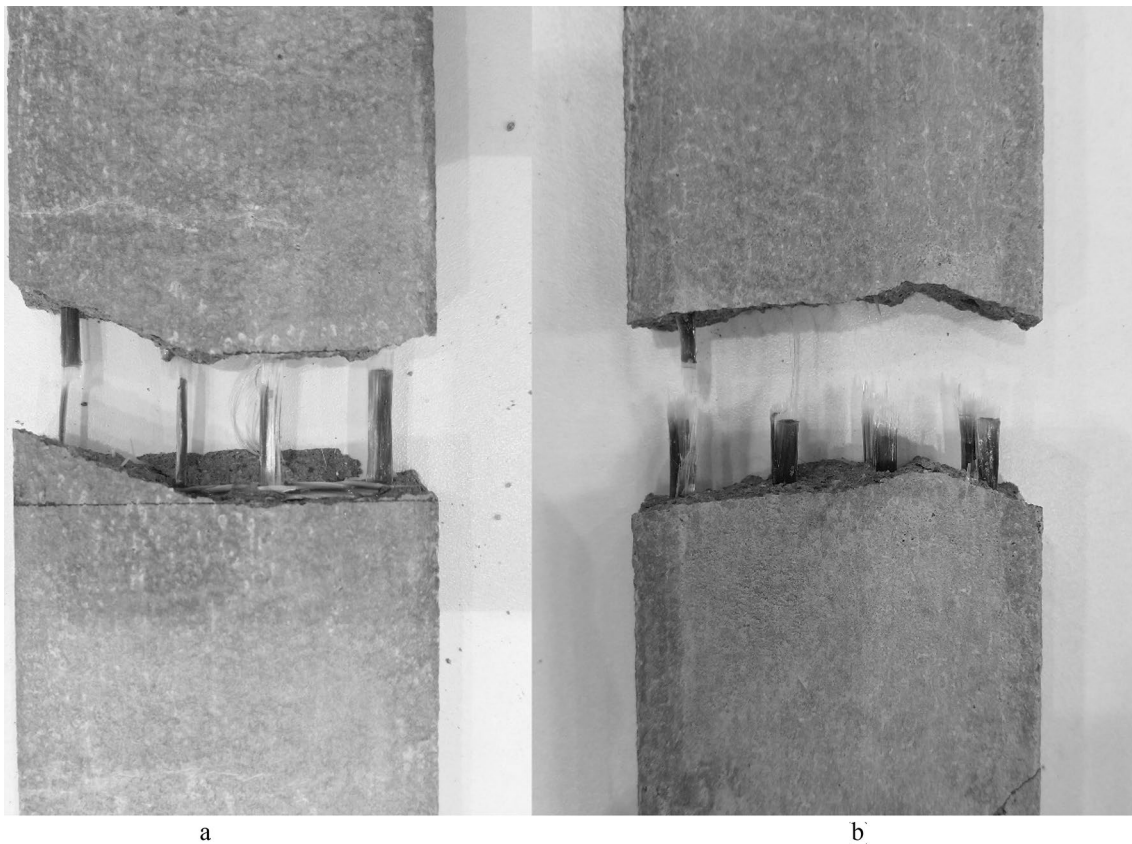


Fig. 8 The failure mode of tensile bond tests: **a** failure mode of Group B specimens; **b** failure mode of Group C specimens.

double time cord-to-matrix interlocking, than by placing the two layers of fabric together. After the first crack appeared near the middle position, the specimens also had another 4–5 cracks spaced 4–7 cm apart, which developed from the middle and extended to the loading ends. After the specimens developed enough cracks, all of them obtained a similar mode of final failure as shown in Fig. 8. The rupture of the fabric near the loading end was the most typical one in the tensile tests using the clamp method.

3.2 Results of the Shear Bond Tests

Before starting the loading, we zeroed the tester data to remove the gravity of the upper prism and frame. The displacement was the average value of the four bond areas of one specimen measured using extensometers. In addition, a half load was used to ascertain the relationship with displacement as two bond laps were used to transfer the tensile load to the bond areas. Once damage had occurred, the loading was stopped. Therefore, under the assumption that the specimen was perfectly vertical and the bond laps on both sides were equally loaded, each stage and bond area were

subjected to a half load from the test machine. Strain gauges were used for the matrix of two specimens, and it was found that the strain at the loading end was greater than that at the free end, but the maximum strain was obtained at the first mortar joint. Due to individual differences in the specimens, the failure of each sample occurred at different bond laps or different bond areas, at random. The typical failure modes are shown in Fig. 9. Further discussion of the results will be presented in conjunction with the various failure modes of the test specimens.

4 Failure Mechanisms

4.1 Fabric-to-Matrix Bond Mechanism

As a reinforcing member responsible for tensile force, the fabric-to-matrix bond is divided into four functions.

The fibre-to-mortar chemical bond is due to the adhesion of the mortar to the surface of the fibres during the crystallisation process. It depends on the chemical nature of the two materials. This function only exists before the relative slippage occurs between the fibres and the matrix. Once a relative slip occurs, this means that the chemical bond has

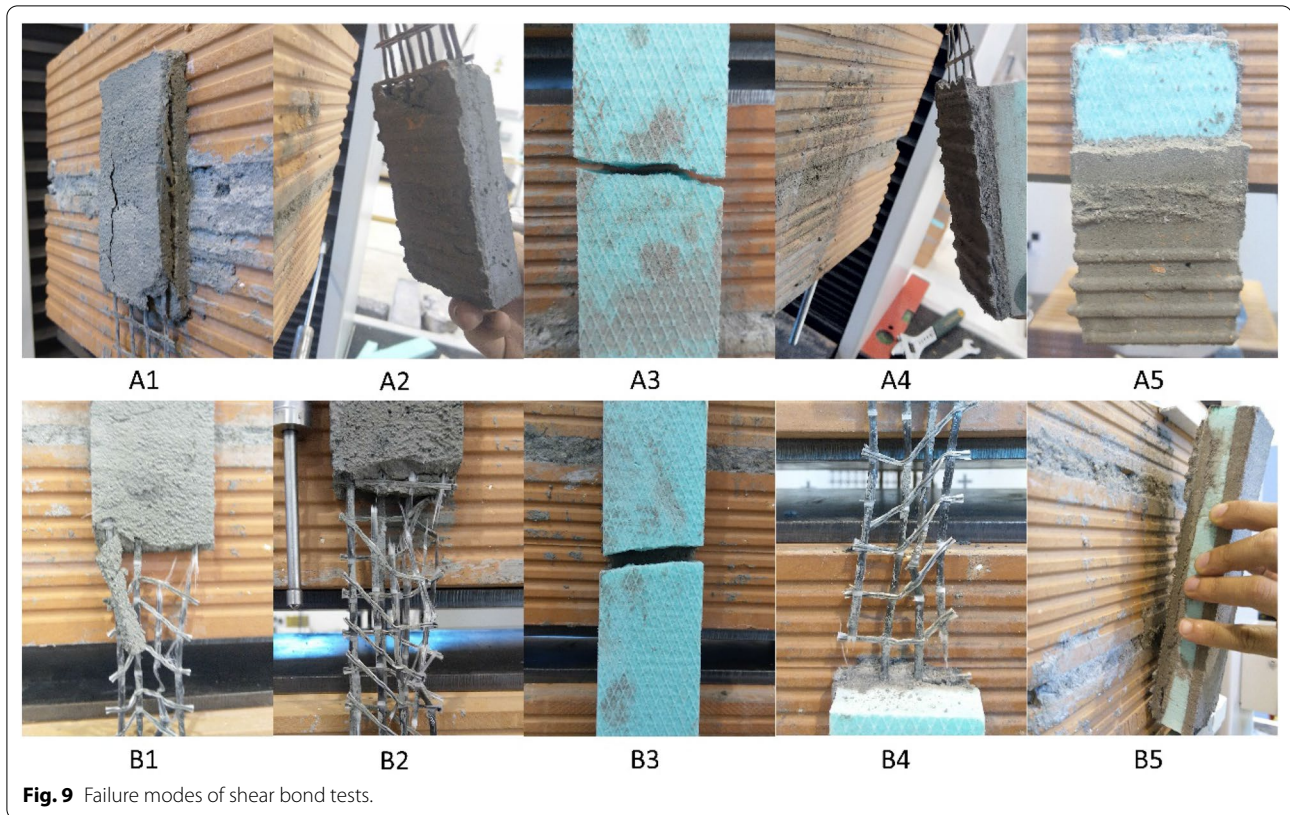


Fig. 9 Failure modes of shear bond tests.

already been destroyed; this failure is irreversible. The fibre (bundle)-to-mortar internal friction is divided into static friction (before the slip) and dynamic friction (during the slip phase). The friction factors often depend on the characterisation of the fibre surface, the strength and hardness of the mortar as well as the gripping method used in the tensile tests. Furthermore, owing to the smooth surface of the fibres, friction can be enhanced by surface preparation such as coating. Bundle-to-cord fastening depends on how the nodes are created—it can also be called a yarn-to-yarn bond if bonded textile is used. Regardless of the type of fabric, a common function is to prevent the main bundles from shifting with the cords in order to avoid further sliding of the bundles. Using bundle-to-cord fastening, the tensile force is transferred to the cords to start cutting the matrix that will produce a large cord-to-mortar mechanical interlocking effect. This function depends on the tensile and shear strengths of the mortar.

4.2 Matrix-to-Substrate Bond Mechanism

The matrix-to-substrate bond is attributed to the chemical bond between the mortar and bricks, which is

applied by the penetration of the mortar into the bricks (and parts of the mortar joints) and the adhesion to the surface. Since debonding occurs in an instant, no normal pressure is applied to the bond area. Therefore, no relative slip frictional resistance is generated. When the shear force is transferred to the grooves on the bricks, the shear strength of the mortar edges in the grooves bears part of the shear load, resulting in mechanical interlocking. Therefore, the viscosity, density, strength of the mortar, and the strength and surface characterisation of the bricks are the factors contributing to the matrix-to-substrate bond.

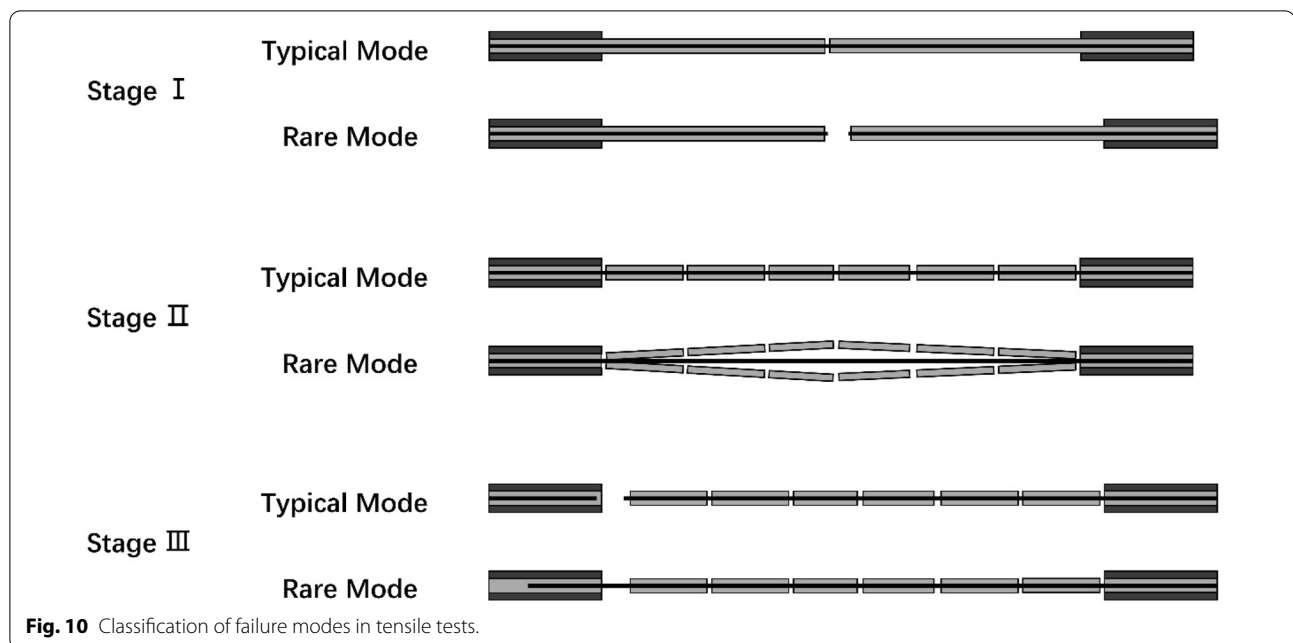
4.3 Matrix-to-Insulation Bond Mechanism

This mechanism should be similar to the matrix-to-substrate bond mechanism, which has a chemical bond as well as mechanical interlocking by the grooves on the surface of the XPS plates.

5 Failure Modes Analysis

5.1 Tensile Bond Tests

A new method is proposed to explain the failure modes of FRCM composites by analysing the fabric-to-matrix



mechanism. The classification of the failure modes in tensile tests is shown in Fig. 10.

In Stage I, the matrix does not break when the composite is subjected to a small tensile force. The fabric does not slip within the matrix, which maintains the optimum fabric-to-matrix bond during this period. The first crack usually occurs in the middle of the specimen if the stress distribution is uniform. If the tensile strength of the fabric is sufficiently large or there is a sufficient number of bundles in the composite, the tensile stress will be further transferred through the principal bundles without breaking the fabric in a one-time splitting. A rare failure mode may be obtained at the end of Stage I, as in Mode A of Caggegi, Lanoye, et al. (2017)), due to low strength in most cases, or a small quantity of fibres in one bundle, or perhaps a few bundles in the matrix.

Subsequently, dynamic friction begins to take effect from Stage II, and as the fibre-to-mortar chemical bond and bundle-to-mortar static friction tends to be small, they cannot prevent the main bundle from slipping. After the tensile stress has been further transmitted to the nodes, it will be transferred by bundle-to-cord fastening to the cords, after which cord-to-mortar mechanical interlocking will begin. This will be strong enough to make the matrix crack, step by step, until the gripping areas are reached. This is called the crack mode of the matrix. Usually, the mortar has a large enough penetration area in the meshes of the fabric so that the matrix only splits during the tension process, unless the composite has a unique failure mode—such as Mode D of Caggegi, Lanoye, et al. (2017)), which is the separation

mode of the matrix due to the small-grid and dense fabric being used.

When the stress and strain of the fabric are transmitted to the gripping areas, the FRCM composite enters the final destruction stage, that is, Stage III. The fabric often exhibits two failure modes. If the fabric-to-matrix bond force in the gripping area is greater than the tensile force that the principal bundles of the fabric can bear, it leads to the occurrence of fabric rupture. Its peak force depends only on the tensile strength of the textile. However, in the glued gripping tests, the tensile failure of the fabric may often be exhibited in the middle of the specimen, yet in the experiments using the clamping method, the rupture of the bundles mostly occurs near the clamp, as was the case in this research. This is because the clamp exerts pressure on the matrix, which increases the bundle-to-mortar friction coefficient, resulting in the bundles achieving maximum strain and stress concentration effects near the clamp. Moreover, if the tensile strength of the fabric is large, the fabric-to-matrix bond will eventually fail, causing the main bundles to exhibit slippage inside the mortar and be pulled from the gripping area of the matrix. This mode is called the slip failure of the fabric, which is more common in glued grips. Its peak force depends on the strength of the bundle-to-cord fastening. The residual bond after the peak force stages of failure is due to the bundle-to-mortar dynamic friction, not dissimilar to the pull-out tests.

Owing to the failure mode of the composites by tensile bond tests, we can use the peak load to calculate the tensile strength of the fabric, as shown in Table 3. From the

Table 3 Strength calculation of all direct tensile tests

Group	No.	Peck load (N)	Strength (MPa)
A (one layer of fabric)	1	3050.79	381.35
	2	2382.26	297.78
	3	2000.81	250.10
	4	2697.53	337.19
	5	2738.13	342.27
	Avg	2573.90	321.74
B (one layer of fabric inside matrix)	1	2371.37	296.42
	2	3239.58	404.95
	3	2731.12	341.39
	4	2612.30	326.54
	5	2695.02	336.88
	Avg	2729.88	341.23
C (two layers of fabric inside matrix)	1	4383.08	273.94
	2	5684.14	355.26
	3	5081.63	317.60
	4	4945.75	309.11
	5	5249.56	328.10
	Avg	5068.83	316.80
The average strength of all specimens			326.59

test results, it was found that the average tensile strength of Group A was slightly higher than that of the single bundles. This was due to the different gripping methods used and the different load transfer media. The same finding was reported in Caggegi, Lanoye, et al. (2017)). Moreover, the results from Groups B and C were similar to those of Group A. This proved that when the composites finally underwent a rupture of the fabric, the ultimate load-bearing capacity depended only on the tensile strength of the fabric.

5.2 Shear Bond Tests

In shear bond tests, the tensile load was exerted as a shear force on the interface between the matrix and bricks by the matrix-to-substrate bond mechanism. Its reaction force is formed by the direct tensile load on the fabric of the unbonded areas, and the tensile stress is transferred into the matrix, producing the fabric-to-matrix bond force. In this research, four failure modes of all specimens were observed, as shown in Fig. 11.

Brittle failure of the matrix (A1): the fabric slipped inside the matrix and the matrix was vertically cut by the fabric (cords) at the end. This means that the bundle-to-cord fastening and matrix-to-substrate bond were

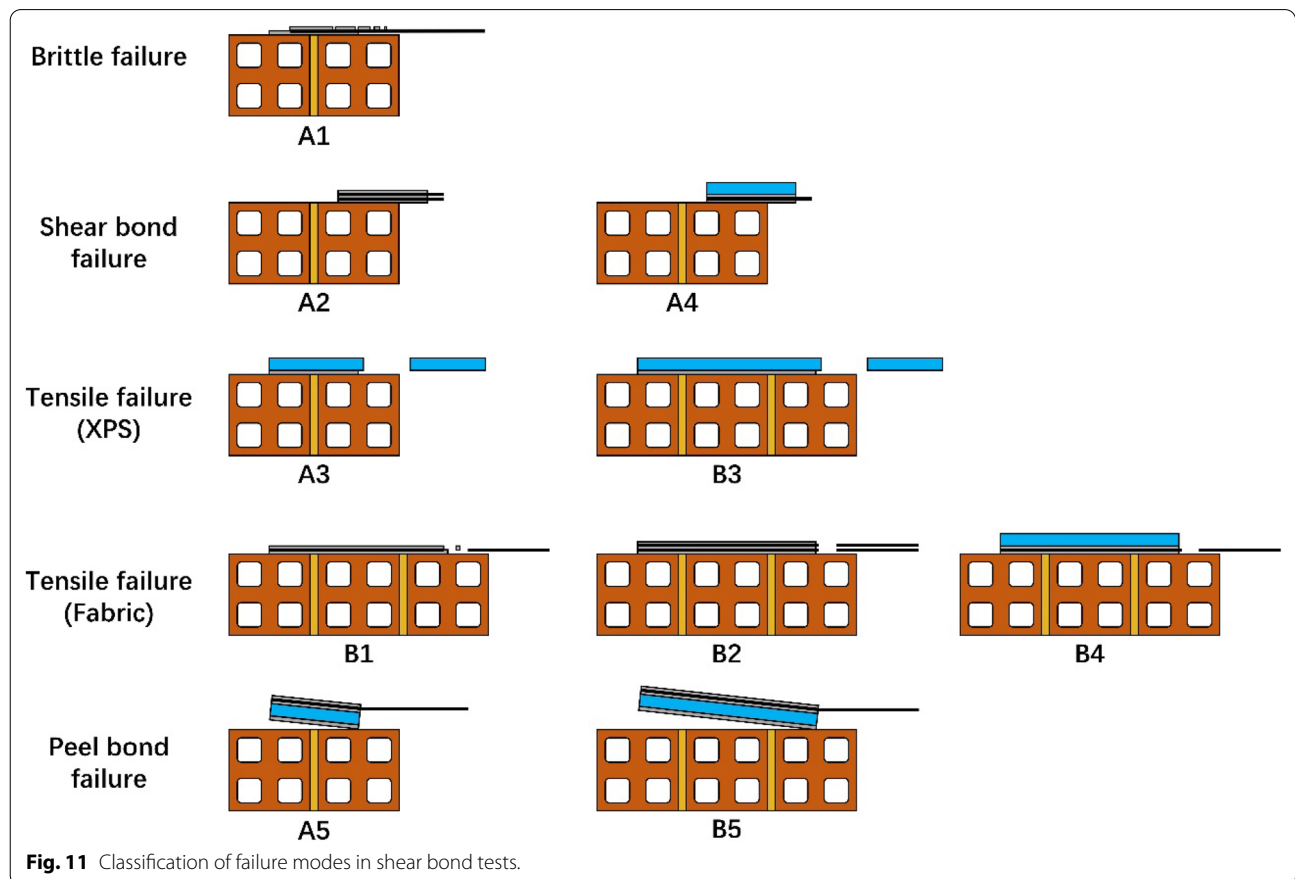


Fig. 11 Classification of failure modes in shear bond tests.

sufficiently secure, but the tensile strength of the mortar was small, or there were no large enough penetration areas in the meshes, so the cords cut the matrix into two parts. The outboard matrix gradually broke from the loading end to the free end, but finally disintegrated in a moment. Here, the peak force depends on the shear strength of the mortar.

Shear bond failure (A2 and A4): debonding occurred gradually between the matrix and substrate from the loading end to the free end owing to the low matrix-to-substrate bond strength. Moreover, the matrix was not damaged. The peak force depends on the shear bond strength between the matrix and the bricks.

Tensile failure of fabric (B1 and B2 and B4) or XPS (A3 and B3): the fabric or XPS plate was pulled off and the matrix may have horizontal cracks near the loading end. The peak force depends on the tensile strength of the material.

Peel bond failure (A5 and B5): debonding occurred between the matrix and substrate from the free end to the loading end. Because the parallel spacing between the fabric and the bond interface was too large, the mortar block at the loading end acted as a fulcrum to convert the load into a twist that caused the free end to be picked off. The peak force depends on the peel bond strength, which is based on the tensile bond strength with a torsional moment.

The brittle failure of the matrix may only occur in the shear bond tests because, in the tensile bond tests the clamped force or rigidity of the grips protect the matrix in the gripping areas from damage. Moreover, two other failure modes may also exist in the shear bond experiments: one is the slip failure of the fabric, which has the same failure mechanism as in the tensile bond tests; the other is the shear failure of the substrate, which may be due to the use of low-strength bricks.

Finally, failure is always produced at the position where the load-bearing capacity is the weakest, which causes the related failure mode to occur. The relevant strengths can be calculated from:

$$P = n \times \min \begin{cases} \sigma_{sb} A_b (1) \\ \sigma_{pb} A_b (2) \\ f_{s,m} A_b (3) \\ f_{t,f} A_{c,f} (4) \end{cases},$$

where n is the number of bond laps of the specimen, σ_{sb} is the shear bond strength, σ_{pb} is the peel bond strength, $f_{s,m}$ is the shear strength of the matrix, $f_{t,f}$ is the tensile strength of the fabric, A_b is the bond area, and $A_{c,f}$ is the cross-sectional area of the fabric.

The strengths of all specimens are listed in Table 4 based on their failure modes. They are empirical and are based on the assumption of elastic response. For

example, for significant components the bond stress is extended exponentially. However, in this test, because the bond length is small, the average strength is used to simplify the calculation so as to compare its strength with that of other failure modes. The shear strength of the mortar is calculated using the longitudinal sectional area of the matrix, which is equivalent to ignoring the area of the fabric in the matrix.

In Setting A2, only the matrix of A2-2 had a partial shear failure of the mortar in the grooves near the loading end. However, after the shear load was transferred over the mortar joint, debonding only occurred at the interface. This might have happened due to faulty production, which may have lowered the mortar strength. B2-2 had a special failure mode in which the inside layer of the fabric was pulled off and the outside layer of the textile cut the matrix. This may have been due to the difference in the tensile prestress applied to the two layers of fabric during the preparation of the test piece. Another possibility is that the outer fabric was left with insufficient mortar protective layer thickness. However, this did not influence the test value much.

Debonding in A5 specimens occurred between the mortar and substrate from the free end to the loading end, at the beginning of the test. However, after the shear load was transmitted over the mortar joint of the substrate, the crack occurred instantly at the interface between the mortar and the XPS layer. Because the rate of break occurred very quickly, the stress could not be transmitted along with the interface in time.

Through the differences between Groups A and B, we successfully changed the failure modes by increasing the bond length and providing sufficient bonding force to pull the fabric off. This also demonstrates that the bond length remains an essential factor in the design of shear bond experiments.

Arrangement A3 was expected to obtain the matrix-to-insulation bond strength. However, all A3 and B3 specimens exhibited tensile failure due to the low tensile strength of the XPS plate (a tensile crack occurred in the middle of the XPS plates).

By comparison with A1, the peak load of A4 was lower, and the failure mode changed too. It can be considered that the XPS plate is as a reinforcement to the matrix, and influences the internal transmission of stress. The matrix and XPS layer were not stripped so that they could be considered as a whole member. Subsequently, the load was further transmitted to the bond interface with the bricks. This led to an interesting result: the matrix was enhanced by the XPS layer, and the failure mode changed, but the peak force was reduced.

Although the standard deviation of the bond strength was significant, the results of specimens A2 and A4

Table 4 Strength calculation of all shear bond tests according to different failure modes

Failure mode	Specimen	Peak load (N)	Half peak load (N)	Section area	Strength (MPa)		
Brittle failure of the matrix	A1-1	4570.01	2285.00	56.8 mm × 110 mm	0.37		
	A1-2	4786.65	2393.32		0.38		
	A1-3	4837.04	2418.52		0.39		
	Avg	4731.23	2365.61		0.38		
Shear bond failure	A2-1	10,278.66	5139.33	56.8 mm × 110 mm	0.82		
	A2-2	6785.30	3392.65		0.54		
	A2-3	8869.21	4434.61		0.71		
	Avg	8644.39	4322.20		0.69		
	Tensile failure of XPS	A4-1	4123.15	2061.57	56.8 mm × 110 mm	0.33	
		A4-2	2998.88	1499.44		0.24	
		A4-3	1756.34	878.17		0.14	
		Avg	2959.46	1479.73		0.24	
		A3-1	713.28	356.64		56.8 mm × 20 mm	0.31
		A3-2*	491.22	245.61			0.22
A3-3	–	–	–				
Tensile failure of fabric	B3-1	719.87	359.94	4 × 2 mm ²	0.32		
	B3-2	825.49	412.75		0.36		
	B3-3	802.26	401.13		0.35		
	Avg	765.23	382.61		0.34		
	Tensile failure of fabric	B1-1	6958.09	3479.05	4 × 2 mm ²	434.88	
		B1-2	7635.88	3817.94		477.24	
		B1-3	7474.90	3737.45		467.18	
		Avg	7356.29	3678.15		459.77	
		Tensile failure of fabric	B2-1	14,827.73	7413.86	8 × 2 mm ²	463.37
			B2-2	15,117.86	7558.93		472.43
			B2-3	13,711.93	6855.96		428.50
			Avg	14,552.51	7276.25		454.77
		Tensile failure of fabric	B4-1	7571.36	3785.68	4 × 2 mm ²	473.21
			B4-2	7650.38	3825.19		478.15
B4-3	7707.60		3853.80	481.72			
Avg	7643.11		3821.56	477.69			
Peel bond failure	A5-1		231.40	115.70	56.8 mm × 110 mm		0.02
	A5-2		1663.16	831.58			0.13
	A5-3	307.08	153.54	0.02			
	Avg	733.88	366.94	0.06			
	Peel bond failure	B5-1	1128.62	564.31	56.8 mm × 220 mm	0.05	
		B5-2	2340.80	1170.40		0.09	
		B5-3	3054.00	1527.00		0.12	
		Avg	2174.48	1087.24		0.09	

* Denotes invalid data because the XPS plate was corroded by glue

– Denotes lost data because the specimen was damaged during placement

indicate that the bond strength was not only determined by the strength of the mortar but also by the strength of the overall matrix. This is consistent with the test results for the first cracks in the tensile bond tests. When two layers of textiles are added to enhance the overall

strength of the composites, the matrix-to-substrate bond strength is also improved.

Moreover, the settings of A5 and B5 failed because of the experimental design, and these should not be used further for the shear bond test as the load transfer was unusual, which led to the peel bond failure.

Consequently, it only reveals that the fabric should not connect two sides of the expansion joint in a building.

6 Conclusions

Through a series of continuous experiments in this study, the following conclusions can be made:

- (1) The tested tensile strength of the fabric is affected not only by the experimental gripping methods, but also by the load transfer and the medium.
- (2) The tensile strength from the first crack of the composite and the shear bond strength are not only determined by the strength of the mortar, but also by the strength of the overall matrix. They should be analysed using the fabric-to-matrix and the matrix-to-substrate bond mechanisms.
- (3) If the thermal insulation does not debond with the matrix, the tensile strength of the XPS plate may be converted to the matrix using a specific coefficient through the matrix-to-insulation bond mechanism, which will enhance the overall strength of the matrix as well as change the failure mode in the shear bond test.

Due to the difference of loading direction, fixation mode and transfer medium, the relationships between the strength measurement results of each material are as follows:

- (4) The test results of mortar blocks show that the flexural strength, tensile strength and the tensile strength after fracture are 11.03%, 3.06% and 2.90% of the compressive strength, respectively. Among them, the tensile strength of mortar blocks is 85.80% (of one layer of fabric inside) and 67.94% (of two layers of fabric inside) of tensile bond test specimens when the first crack occurs.
- (5) The tensile strengths of fabric in different test methods show that the results of the single bundle tensile tests and tensile bond tests are 62.42% and 70.37% of the results of the tensile failure of fabric in shear bond tests, respectively.

7 Further Discussion

The matrix-to-insulation bond strength was not tested in this experiment, but it does not need to be independently studied on this new upgrading system for masonry walls due to the low strength of XPS. If the FRM is used as the outer layer, it may cause shear bond failure in the matrix-to-insulation interface or shear failure in the XPS layer. Therefore, it is an unreasonable setting. However, if the FRM is set in the middle, between the thermal insulation and the substrate, the XPS plate always cracks

together with the matrix without being debonded, especially on a large-scale wall of sufficient bond length.

Moreover, although we obtained a good result for the fabric-to-matrix bond of FRM composites, several research studies on large-scale experiments have similar results that demonstrate that the FRM overlay debonded from the wall due to in-plane loading, because of the low matrix-to-substrate bond strength. This means that the FRM system will undergo shear bond failure and the overlay will ultimately lose its functionality, causing the wall to be easily destroyed. It is known that the most desirable failure mode is that of the FRM composite cracking together with the wall without being debonded, but this expectation may not be fully realised. However, by correctly adding shear connectors between the masonry wall and the FRM composites, or making shallow grooves on the surface of the wall, or by setting anchors to connect the overlay to RC frames, it is possible to prevent bond failure from occurring prematurely. Based on the above discussion, the FRM system can be expected to provide more lasting protection for the wall, thereby achieving substantial improvement.

To summarise, the focus of further research will be on how to properly arrange the layers of materials while choosing an effective measure to increase the shear bearing between the interfaces. It will be necessary to perform experiments using cyclic loading on large-scale masonry wall infill RC frames retrofitted with both FRM composites and thermal insulation to verify this new system.

Acknowledgements

Not applicable

Authors' contributions

CC conceived the experiment; FW and NK designed the experiment; FW and NK purchased the materials; FW and EE manufactured the specimens; FW and EE tested the data; NK, RV and RI helped the tests; FW analysed and interpreted the data; FW wrote the manuscript; FW and NK revised the manuscript. All authors read and approved the final manuscript.

Authors' information

FW, Ph.D. Candidate, Email: Fayu_Wang@outlook.com (corresponding author), Research Fellow at Department of Civil Engineering and Geomatics, Faculty of Engineering and Technology, Cyprus University of Technology.

NK, Ph.D., Email: nicholas.kyriakides@cut.ac.cy (corresponding author), Lecturer at Department of Civil Engineering and Geomatics, Faculty of Engineering and Technology, Cyprus University of Technology.

CC, Ph.D., Email: c.chrysostomou@cut.ac.cy, Vice Rector for Economic Planning and Development; Professor at Department of Civil Engineering and Geomatics, Faculty of Engineering and Technology, Cyprus University of Technology, Cyprus University of Technology.

EE, M.E., Email: Lefteriselef@hotmail.com, Research Associate at Department of Civil Engineering and Geomatics, Faculty of Engineering and Technology, Cyprus University of Technology.

RV, Ph.D., Email: renos.votsis@cut.ac.cy, Post-doctoral Research Fellow at Department of Civil Engineering and Geomatics, Faculty of Engineering and Technology, Cyprus University of Technology.

RI, Ph.D., Email: rilamp01@ucy.ac.cy, Post-doctoral Research Fellow at Department of Civil and Environmental Engineering, University of Cyprus.

Funding

This work was co-funded by the European Regional Development Fund and the Republic of Cyprus through the Research and Innovation Foundation. Project name: SupERB-Novel integrated approach for seismic and energy upgrading of existing buildings (INTEGRATED/0916/0004).

Availability of data and materials

The datasets used and/or analysed during the current study are available from the corresponding author on reasonable request.

Declarations

Competing interests

The authors declare that they have no competing interests.

Author details

¹Research Fellow, Department of Civil Engineering and Geomatics, Faculty of Engineering and Technology, Cyprus University of Technology, No. 30 Archiepiskopou Kyprianou Str., P.O. Box 50329, 3036 Limassol, Cyprus. ²Lecturer, Department of Civil Engineering and Geomatics, Faculty of Engineering and Technology, Cyprus University of Technology, No. 30 Archiepiskopou Kyprianou Str., P.O. Box 50329, 3036 Limassol, Cyprus. ³Vice Rector for Economic Planning and Development; Professor, Department of Civil Engineering and Geomatics, Faculty of Engineering and Technology, Cyprus University of Technology, No. 30 Archiepiskopou Kyprianou Str., P.O. Box 50329, 3036 Limassol, Cyprus. ⁴Research Associate, Department of Civil Engineering and Geomatics, Faculty of Engineering and Technology, Cyprus University of Technology, No. 30 Archiepiskopou Kyprianou Str., P.O. Box 50329, 3036 Limassol, Cyprus. ⁵Post-doctoral Research Fellow, Department of Civil Engineering and Geomatics, Faculty of Engineering and Technology, Cyprus University of Technology, No. 30 Archiepiskopou Kyprianou Str., P.O. Box 50329, 3036 Limassol, Cyprus. ⁶Post-doctoral Research Fellow, Department of Civil and Environmental Engineering, University of Cyprus, 75 Kallipoleos Str., P.O. Box 20537, 1678 Nicosia, Cyprus.

Received: 12 November 2020 Accepted: 5 April 2021

Published online: 29 April 2021

References

- Ac434 I (2013). Acceptance criteria for masonry and concrete strengthening using fiber-reinforced cementitious matrix (FRCM) composite systems. ICC-Evaluation Service, Whittier, CA
- ACI Committee 549. (2013). 549.4R-13 Guide to design and construction of externally bonded Fabric-Reinforced Cementitious Matrix (FRCM) systems for repair and strengthening concrete and masonry structures. Farmington Hills, MI: American Concrete Institute. https://www.concrete.org/store/productdetail.aspx?ItemID=549413&Format=DOWNLOAD&Language=English&Units=US_AND_METRIC
- Aggarwal, L., Thapliyal, P., & Karade, S. (2007). Properties of polymer-modified mortars using epoxy and acrylic emulsions. *Construction and Building Materials*, 21, 379–383.
- Arboleda, D., Carozzi, F. G., Nanni, A., et al. (2016). Testing procedures for the uniaxial tensile characterization of fabric-reinforced cementitious matrix composites. *Journal of Composites for Construction*, 20, 04015063.
- Ascione, L., De Felice, G., & De Santis, S. (2015). A qualification method for externally bonded Fibre Reinforced Cementitious Matrix (FRCM) strengthening systems. *Composites Part B: Engineering*, 78, 497–506.
- Blanksvärd, T., Täljsten, B., & Carolin, A. (2009). Shear strengthening of concrete structures with the use of mineral-based composites. *Journal of Composites for Construction*, 13, 25–34.
- Butler, M., Mechtcherine, V., & Hempel, S. (2010). Durability of textile reinforced concrete made with AR glass fibre: Effect of the matrix composition. *Materials and Structures*, 43, 1351–1368.
- Caggegi, C., Carozzi, F. G., De Santis, S., et al. (2017). Experimental analysis on tensile and bond properties of PBO and aramid fabric reinforced cementitious matrix for strengthening masonry structures. *Composites Part B: Engineering*, 127, 175–195.
- Caggegi, C., Lanoye, E., Djama, K., et al. (2017). Tensile behaviour of a basalt TRM strengthening system: Influence of mortar and reinforcing textile ratios. *Composites Part B: Engineering*, 130, 90–102.
- Carozzi, F. G., & Poggi, C. (2015). Mechanical properties and debonding strength of Fabric Reinforced Cementitious Matrix (FRCM) systems for masonry strengthening. *Composites Part B: Engineering*, 70, 215–230.
- D3039/D3039M-17 (2017). Standard test method for tensile properties of polymer matrix composite materials. Standard test method for tensile properties of polymer matrix composite materials. ASTM International
- Dalalbashi, A., Ghiassi, B., Oliveira, D. V., et al. (2018). Fiber-to-mortar bond behavior in TRM composites: Effect of embedded length and fiber configuration. *Composites Part B: Engineering*, 152, 43–57.
- D'antino, T., & Papanicolaou, C. (2018). Comparison between different tensile test set-ups for the mechanical characterization of inorganic-matrix composites. *Construction and Building Materials*, 171, 140–151.
- De Felice, G., D'antino, T., De Santis, S., et al. (2020). Lessons learned on the tensile and bond behavior of fabric reinforced cementitious matrix (FRCM) composites. *Frontiers in Built Environment*. <https://doi.org/10.3389/fbuil.2020.00005>.
- De Santis, S., & De Felice, G. (2015). Tensile behaviour of mortar-based composites for externally bonded reinforcement systems. *Composites Part B: Engineering*, 68, 401–413.
- De Felice, G., Aiello, M. A., Bellini, A., et al. (2016). Experimental characterization of composite-to-brick masonry shear bond. *Materials and Structures*, 49, 2581–2596.
- De Felice, G., Aiello, M. A., Caggegi, C., et al. (2018). Recommendation of RILEM Technical Committee 250-CSM: Test method for Textile Reinforced Mortar to substrate bond characterization. *Materials and Structures*, 51, 95.
- De Santis, S., Carozzi, F. G., De Felice, G., et al. (2017). Test methods for textile reinforced mortar systems. *Composites Part B: Engineering*, 127, 121–132.
- De Santis, S., Ceroni, F., De Felice, G., et al. (2017). Round Robin Test on tensile and bond behaviour of Steel Reinforced Grout systems. *Composites Part B: Engineering*, 127, 100–120.
- Jiang, J., Jiang, C., Li, B., et al. (2019). Bond behavior of basalt textile meshes in ultra-high ductility cementitious composites. *Composites Part B: Engineering*, 174, 107022.
- Kim, H.-S., Truong, G.T., Park, S.-H. et al. (2018). Tensile Properties of Carbon Fiber-Textile Reinforced Mortar (TRM) Characterized by Different Anchorage Methods. *International Journal of Concrete Structures and Materials* 12
- Krishnamurthy, B. S., Balamuralikrishnan, R., & Shakil, M. (2017). An experimental work on alkaline resistance glass fiber reinforced concrete. *International Journal of Advanced Engineering, Management and Science*, 3, 730–737.
- Larrinaga, P., Chastre, C., Biscaia, H. C., et al. (2014). Experimental and numerical modeling of basalt textile reinforced mortar behavior under uniaxial tensile stress. *Materials & Design*, 55, 66–74.
- Orosz, K., Blanksvärd, T., Täljsten, B., et al. (2010). From material level to structural use of mineral-based composites—an overview. *Advances in Civil Engineering*, 2010, 1–19.
- Scheffler, C., Gao, S. L., Plonka, R., et al. (2009a). Interphase modification of alkali-resistant glass fibres and carbon fibres for textile reinforced concrete I: Fibre properties and durability. *Composites Science and Technology*, 69, 531–538.
- Scheffler, C., Gao, S. L., Plonka, R., et al. (2009b). Interphase modification of alkali-resistant glass fibres and carbon fibres for textile reinforced concrete II: Water adsorption and composite interphases. *Composites Science and Technology*, 69, 905–912.
- Signorini, C., Nobili, A., Cedillo González, E. I., et al. (2018). Silica coating for interphase bond enhancement of carbon and AR-glass Textile Reinforced Mortar (TRM). *Composites Part B: Engineering*, 141, 191–202.
- Triantafyllou, T. C., Karlos, K., Kefalou, K., et al. (2017). An innovative structural and energy retrofitting system for URM walls using textile reinforced mortars combined with thermal insulation: Mechanical and fire behavior. *Construction and Building Materials*, 133, 1–13.
- Triantafyllou, T. C., Karlos, K., Kapsalis, P., et al. (2018). Innovative structural and energy retrofitting system for masonry walls using textile reinforced

mortars combined with thermal insulation: In-plane mechanical behavior. *Journal of Composites for Construction*, 22, 04018029.
Uni, E (2019). 1015-11: 2019. Methods of test for mortar for masonry-Part 11

Publisher's Note

Springer Nature remains neutral with regard to jurisdictional claims in published maps and institutional affiliations.

Submit your manuscript to a SpringerOpen[®] journal and benefit from:

- ▶ Convenient online submission
- ▶ Rigorous peer review
- ▶ Open access: articles freely available online
- ▶ High visibility within the field
- ▶ Retaining the copyright to your article

Submit your next manuscript at ▶ [springeropen.com](https://www.springeropen.com)
